J|A|C|S
ARTICLES

Published on Web 10/06/2009

An Electrochemical Sensor for Single Nucleotide Polymorphism Detection in Serum Based on a Triple-Stem DNA Probe

Yi Xiao,*[,†,‡] Xinhui Lou,[†,‡] Takanori Uzawa,[§] Kory J. I. Plakos,[‡] Kevin W. Plaxco,[§,||] and H. Tom Soh*[,†,‡,||]

Materials Department, Department of Mechanical Engineering, Department of Chemistry and Biochemistry, Program in BioMolecular Science and Engineering, University of California, Santa Barbara, California 93106

Received June 26, 2009; E-mail: yixiao@physics.ucsb.edu; tsoh@engineering.ucsb.edu

Abstract: We report here an electrochemical approach that offers, for the first time, single-step, room-temperature single nucleotide polymorphism (SNP) detection directly in complex samples (such as blood serum) without the need for target modification, postwashing, or the addition of exogenous reagents. This sensor, which is sensitive, stable, and reusable, is comprised of a single, self-complementary, methylene blue-labeled DNA probe possessing a triple-stem structure. This probe takes advantage of the large thermodynamic changes in enthalpy and entropy that result from major conformational rearrangements that occur upon binding a perfectly matched target, resulting in a large-scale change in the faradaic current. As a result, the discrimination capabilities of this sensor greatly exceed those of earlier single- and double-stem electrochemical sensors and support rapid (minutes), single-step, reagentless, room-temperature detection of single nucleotide substitutions. To elucidate the theoretical basis of the sensor's selectivity, we present a comparative thermodynamic analysis among single-, double-, and triple-stem probes.

Introduction

Tools for accurate, sequence-specific DNA analysis are essential for understanding the association between genetics, heritable phenotypes, and drug responses.[1a,b] One critical application is the detection of single nucleotide polymorphisms (SNPs), which are important biomarkers for genetic diseases[1c] and are implicated in disease mechanisms of cancer and diabetes.[1d] Likewise the detection of rare base substitutions within populations of DNA molecules is of value in studies of DNA damage and in pool screening for SNPs.[1e] Thus motivated, a variety of optical methods have been developed to date for the specific detection of SNPs, including enzymatic probes,[2] molecular beacons,[3,4] and binary probes.[5] However, such methods suffer from several drawbacks, including the relative complexity inherent in optical imaging/detection methodologies, low specificity at room temperature,[3,4] and potential interference arising from contaminating fluorophores, quenchers, or colorants.[6] Electrochemical approaches, in contrast, exhibit relatively low background and readily integrate with microelectronics. Given these benefits, electrochemical sensors could be well suited for point-of-care SNP analysis in complex samples.[7]

A number of electrochemical DNA sensors for SNP analysis have been recently reported.[8−12] For example, Barton et al. described a system that detects changes in long-range charge transport though the π-stack of duplex DNA by combining redox-active intercalators with exogenous electrocatalytic species.[8] In this approach, targets that alter base-pair stacking, such as a mismatched base within the DNA duplex, are identified via reduced charge transfer relative to perfectly matched targets. Other groups have employed electrochemically active DNA probes in a variety of SNP analysis strategies, including the posthybridization application of exogenous redox-active reporters with preferential affinity for duplex DNA[9] or sandwich assays based on redox-labeled DNA probes that bind to a target DNA sequence.[10] These approaches offer accurate room-temperature SNP detection but are often susceptible to false positives arising from nonspecific binding of redox reporters and require exogenous reagents and posthybridization washing steps.

[†] Materials Department.
[‡] Department of Mechanical Engineering.
[§] Department of Chemistry and Biochemistry.
[||] Program in BioMolecular Science and Engineering.

(1) (a) Schork, N. J.; Fallin, D.; Lanchbury, J. S. *Clin. Genet.* **2000**, *58*, 250–264. (b) McCarthy, J. J.; Hilfiker, R. *Nat. Biotechnol.* **2000**, *18*, 505–508. (c) Naylo, S. L. *Front. Biosci.* **2007**, *12*, 4111–4131. (d) Akerman, B. R.; Natowicz, M. R.; Kaback, M. M.; Loyer, M.; Campeau, E.; Gravel, R. A. *Am. J. Hum. Genet.* **1997**, *60*, 1099–1106. (e) Luo, J. D.; Chan, E. C.; Shih, C. L.; Chen, T. L.; Liang, Y.; Hwang, T. L.; Chiou, C. C. *Nucleic Acids Res.* **2006**, *34*, e12.
(2) (a) Livak, K. J.; Marmaro, J.; Todd, J. A. *Nat. Genet.* **1995**, *9*, 341–342. (b) Landegren, U.; Kaiser, R.; Sanders, J.; Hood, L. *Science* **1988**, *241*, 1077–1080. (c) Ficht, S.; Mattes, A.; Seitz, O. *J. Am. Chem. Soc.* **2004**, *126*, 9970–9981.
(3) (a) Tyagi, S.; Kramer, F. R. *Nat. Biotechnol.* **1996**, *14*, 303–308. (b) Nutiu, R.; Li, Y. F. *Nucleic Acids Res.* **2002**, *30*, e94.
(4) Grossmann, T. N.; Roglin, L.; Seitz, O. *Angew. Chem., Int. Ed.* **2007**, *46*, 5223–5225.
(5) (a) Xu, Y. Z.; Karalkar, N. B.; Kool, E. T. *Nat. Biotechnol.* **2001**, *19*, 148–152. (b) Kolpashchikov, D. M. *J. Am. Chem. Soc.* **2005**, *127*, 12442–12443. (c) Kolpashchikov, D. M. *J. Am. Chem. Soc.* **2006**, *128*, 10625–10628.
(6) Bowtell, D. D. L. *Nat. Genet.* **1999**, *21*, 25–32.
(7) Willner, I. *Science* **2002**, *298*, 2407–2408.

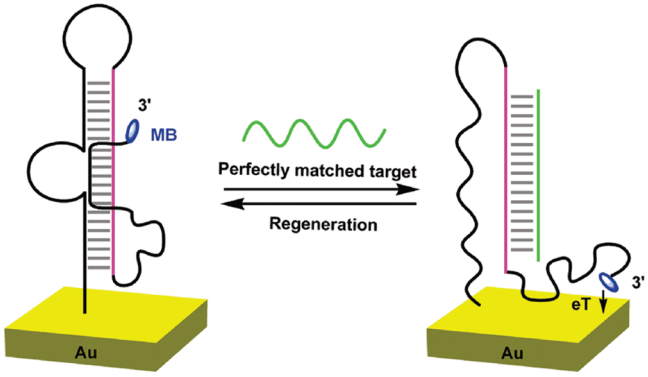

Figure 1. Mechanism of the regenerable E-SNP sensor, wherein detection is based on conformational rearrangement of the triple-stem DNA probe upon binding a perfectly matched target. In the absence of perfectly matched target (left), the triple-stem probe forms a discontinuous, rigid, 21-base duplex, inhibiting electron transfer between the MB redox label and electrode. Upon target binding (right), the triple-stem structure is disrupted, liberating a flexible, single-stranded segment and enabling efficient collisions between the MB and electrode.

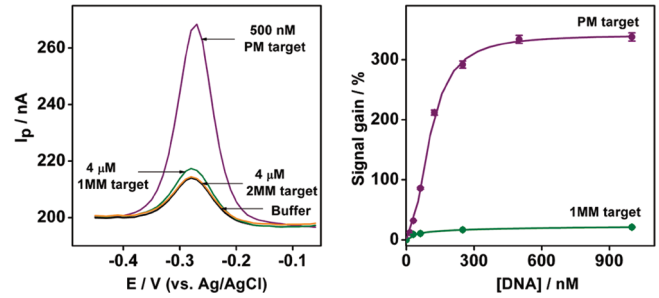

Figure 2. (Left) Alternating current (AC) voltammograms of the E-SNP sensor challenged with either 500 nM of the perfectly matched (PM) target (**2**) or 4 μM of either a single-base (1MM) (**3**) or two-base (2MM) (**4**) mismatched targets. (Right) The E-SNP sensor demonstrates exquisite discrimination against the single-base mismatched target over a broad concentration range. The illustrated error bars represent the standard deviation of five measurements conducted with a single electrode at each concentration; multiple electrodes were used to collect the entire data set. Relative sensor response (%) was employed to normalize for any discrepancies in electrode area and/or surface coverage. All hybridization reactions were performed in 300 μL of solution for 3 h.

Motivated by the limitations of the above-described approaches we report here a single-step electrochemical approach that alleviates these cumbersome requirements and combines for the first time sensitive, room-temperature SNP detection with excellent stability and reusability, without the need for target modification, postwashing, or the addition of exogenous reagents. The electrochemical SNP (E-SNP) sensor is based on a single, redox-labeled DNA strand that incorporates three stems (Figure 1). This triple-stem DNA probe is unique and distinct from previously reported redox-labeled single- (molecular beacon)[11] and double-stem (pseudoknot)[12] DNA probes, which can only distinguish two- or three-base mismatches at room temperature. To elucidate the theoretical basis of SNP selectivity, we present a comparative thermodynamic analysis among single-, double-, and triple-stem probes. In doing so we find that the E-SNP platform takes advantage of the large thermodynamic changes in enthalpy and entropy that result from conformational rearrangement of the triple-stem DNA probe upon binding to a perfectly matched target, giving rise to exquisite sensitivity to single-base mismatches even in the complex medium of blood serum.

Results and Discussion

The E-SNP sensor is comprised of a single DNA element that self-hybridizes into three distinct, seven-base-pair (bp) Watson−Crick stems[13] that form a discontinuous 21-base double helix (Figure 1, left). This triple-stem DNA probe (**1**, 5′-HS-$(CH_2)_{11}$AGGCTGGATTTTTTATTTACCTTTTTTTAGGTAA-AACGACGGCCAGCCTTTTTTTTTTTTTCCGTCGT-$(CH_2)_7$MB-3′) is modified with a redox-active methylene blue (MB) tag at its 3′ terminus and covalently attached to a gold electrode via a thiol group[14] at its 5′ terminus. In the absence of complementary DNA targets, the discontinuous double helix fixes MB away from the electrode (Figure 1, left), and we observe only minimal faradaic current at the formal potential (−0.28 V vs Ag/AgCl) expected for MB (Figure 2, left, buffer). The observed background presumably arises due to limited, long-range electron transfer from folded probes or short-range electron transfer from transiently unfolded probes. Hybridization with a perfectly matched target, however, disrupts the triple-stem structure, liberating a flexible, single-stranded segment encompassing the MB-labeled 3′ terminus of the probe (Figure 1, right). This in turn enables interaction of the redox label with the electrode and increases the observed faradaic current.

At a saturating concentration (≥500 nM) of the 17-base, perfectly matched (PM) target (**2**, 5′-GCTGGCCGTCGTTTTAC-3′), the faradaic current increased by 335 ± 7% (Figure 2, left, PM target). In contrast, a single-base mismatched (1MM) target (**3**, 5′-GCTGGCCCTCGTTTTAC-3′) at an 8-fold higher concentration produced only a 23 ± 1% increase in signal (Figure 2, left, 1MM target), and a two-base mismatched (2MM) target (**4**, 5′-GCTGGCCCCCGTTTTAC-3′) does not produce any measurable (<2%) signal change at concentrations as high as 4 μM (Figure 2, left, 2MM target). This large difference in signal gain suggests that mismatched targets are significantly less capable of disrupting the probe's triple-stem structure relative to PM targets under the room temperature conditions employed. Conversely, we also synthesized a second thiolated, MB-modified triple-stem probe (**5**) with an A-to-G substitution at position 39 (from the 5′ end) such that it perfectly matches the 1MM target (**3**) and is now mismatched with the PM target (**2**). As expected, this modified sensor achieved a 312 ± 5% signal gain in a sample containing 500 nM 1MM target and a 21 ± 1% signal increase with an 8-fold excess (4 μM) of PM

(8) (a) Kelley, S. O.; Boon, E. M.; Barton, J. K.; Jackson, N. M.; Hill, M. G. *Nucleic Acids Res.* **1999**, *27*, 4830–4837. (b) Boon, E. M.; Ceres, D. M.; Drummond, T. G.; Hill, M. G.; Barton, J. K. *Nat. Biotechnol.* **2000**, *18*, 1096–1100. (c) Wong, E. L. S.; Gooding, J. *J. Anal. Chem.* **2006**, *78*, 2138–2144. (d) Inouye, M.; Ikeda, R.; Takase, M.; Tsuri, T.; Chiba, J. *Proc. Natl. Acad. Sci. U.S.A.* **2005**, *102*, 11606–11610.
(9) Wakai, J.; Takagi, A.; Nakayama, M.; Miya, T.; Miyahara, T.; Iwanaga, T.; Takenaka, S.; Ikeda, Y.; Amano, M. *Nucleic Acids Res.* **2004**, *32*, e141.
(10) (a) Yu, C. J.; Wan, Y. J.; Yowanto, H.; Li, J.; Tao, C. L.; James, M. D.; Tan, C. L.; Blackburn, G. F.; Meade, T. J. *J. Am. Chem. Soc.* **2001**, *123*, 11155–11161. (b) Xiao, Y.; Lubin, A. A.; Baker, B. R.; Plaxco, K. W.; Heeger, A. J. *Proc. Natl. Acad. Sci. U.S.A.* **2006**, *103*, 16677–16680. (c) Yamana, K.; Mitsui, T.; Yoshioka, J.; Isuno, T.; Nakano, H. *Bioconjugate Chem.* **1996**, *7*, 715–720.
(11) Lubin, A. A.; Lai, R. Y.; Baker, B. R.; Heeger, A. J.; Plaxco, K. W. *Anal. Chem.* **2006**, *78*, 5671–5677.
(12) (a) Xiao, Y.; Qu, X. G.; Plaxco, K. W.; Heeger, A. J. *J. Am. Chem. Soc.* **2007**, *129*, 11896–11897. (b) Cash, K. J.; Heeger, A. J.; Plaxco, K. W.; Xiao, Y. *Anal. Chem.* **2009**, *81*, 656–661.
(13) Sperschneider, J.; Datta, A. *RNA* **2008**, *14*, 630–640.
(14) Porter, M. D.; Bright, T. B.; Allara, D. L.; Chidsey, C. E. D. *J. Am. Chem. Soc.* **1987**, *109*, 3559–3568.

target (see Supporting Information Figure S1), suggesting that the triple-stem probe achieves this level of discrimination without any significant optimization.

The density with which the immobilized DNA probes are packed on the electrode surface strongly affects the gain of sensors in this class.[15] To explore this phenomenon, we varied the surface coverage by changing the concentrations of the triple-stem DNA probe employed during the electrode preparation step. Testing surface coverages from 2 ± 1 to 65 ± 5 pmol·cm^{-2} we observed optimal signal gain (330 ± 6%) at 35 ± 2 pmol·cm^{-2}, and the gain falls at both lower (81 ± 3% at 5 ± 2 pmol·cm^{-2}) and higher (120 ± 4% at 65 ± 5 pmol·cm^{-2}) densities (data not shown). We presume that this behavior arises due to two competing effects. At high densities, the probes are sterically constrained from forming their native self-complementary structure, which increases short-range electron transfer from the unfolded probes and elevates the background current. At low probe densities, on the other hand, properly folded triple-stem probes may collide with the surface and thereby increase the background current and decrease the net signal gain.

To quantitatively characterize the specificity of the E-SNP sensor, we have defined the single-base mismatch discrimination factor as the ratio of the net signal gain obtained with the PM target to that obtained with the 1MM counterpart (PM gain/1MM gain). A larger discrimination factor is thus indicative of improved specificity. Our sensor achieved a discrimination factor of 8.1 in a comparative analysis of the two targets at concentrations of 64 nM, and robust discrimination capabilities were observed over a wide range of concentrations (Figure 2, right). Notably, the E-SNP sensor retains its excellent discrimination ability at room temperature even in the presence of high concentrations of mismatched target. For example, we obtained a discrimination factor of 4.2 in a sample containing 64 nM PM target and a 62.5-fold excess (4 μM) of 1MM target (Figure 2, right). The titration curve indicates a nonlinear hyperbolic relationship between DNA hybridization efficiency and target concentration, suggesting that the observed signal change is dominated by the hybridization thermodynamics, as described in related reports.[16,17]

To demonstrate the generality of the E-SNP sensor, we have used single-base mismatches at different positions across the 17-base target and observed discrimination factors ranging from 2.7 to 13.8 (Table 1). Among these variants, the best discrimination was observed for a C−C mismatch and the lowest was an A−A mismatch, which correlates well with previous evidence that cytosine mismatches are among the most destabilizing.[18] These experimental results also demonstrated that the thermodynamics of mismatches located in the middle of the target depend on the identity of the mismatched base pair as well as the identity of its adjacent neighbors.[19]

Testing targets of 15 to 19 bases with single nucleotide substitutions located in the middle of each sequence, we find that the exceptional specificity of the E-SNP sensor is retained. We observed only relatively minor differences in signal gain among single-base mismatched targets of 15, 17, and 19 bases in length, and the discrimination factors for these targets were 15.1, 13.4, and 10.3, respectively (Figure 3, left).

Table 1. Discrimination Factors of the Triple-Stem Probe (**1**) for Single-Base Mismatched Targets Differing from the 17-Base PM Target (**2**) (5′-GCTGGCCGTCGTTTTAC-3′) (Mismatches Marked in Red)

DNA Target Sequence (5'---3')	Discrimination factors	Mismatched Base-Pair
GCTGGCCGTCGTTTTAC		
GCTGGGCGTCGTTTTAC	3.9	G-G
GCTGGCGGTCGTTTTAC	6.9	G-G
GCTGGCCCTCGTTTTAC	13.8	C-C
GCTGGCCGACGTTTTAC	2.7	A-A
GCTGGCCGCCGTTTTAC	3.8	A-C
GCTGGCCGGCGTTTTAC	5.9	A-G
GCTGGCCGTGGTTTTAC	7.1	G-G
GCTGGCCGTCCTTTTAC	13.2	C-C
GCTGGCCGTCGCTTTAC	6.2	A-C

The response time of the E-SNP sensor compares favorably to enzyme-mediated SNP detection methods;[8,10] signal saturation is observed after 2.5 h, with 75% of maximum signal achieved within 60 min (Figure 3, right). Even when analyzing samples containing an 8-fold excess of 1MM target relative to PM target, the sensor achieves a discrimination factor of 8 after only 30 min (Figure 3, right). It should be noted that the observed hybridization kinetics of our triple-stem probe are relatively slow compared with single- and double-stem probes,[11,12] which is consistent with the fact that the rate of hybridization is known to be inversely proportional to the thermodynamic stability of the constrained probes.[20,21]

An important advantage of the E-SNP sensor arises from the fact that the sensor is actuated via a target-induced conformational change of the triple-stem DNA probe and is, thus, relatively impervious to false signals arising from nonspecific adsorption of interferants to the sensor surface. As a result, the sensor operates effectively in complex physiological samples. For example, the sensor yielded a 118% signal gain when challenged with a 500 nM 17-base perfectly matched target (**2**) in 50% fetal calf serum (Figure 4, left). In contrast, 4 μM of a single-base mismatched target (**3**) produces only a 10% signal change (Figure 4, left). The reduced gain observed in these

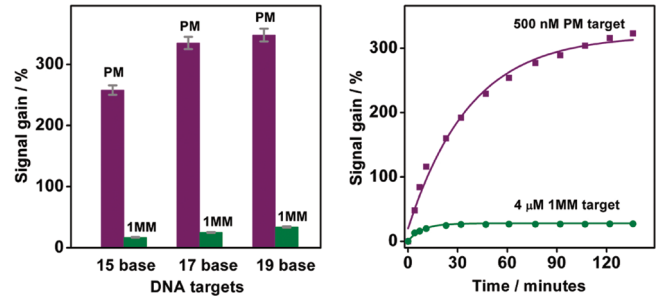

Figure 3. (Left) The discrimination performance of the E-SNP sensor is not diminished for targets of different lengths. All hybridization reactions were performed in 300 μL of solution for 3 h. (Right) Sensor signal reaches 75% of saturation within 60 min for a 500 nM concentration of 17-base PM target (**2**). In contrast, 4 μM 1MM target (**3**) produces negligible signal gain, even after 2 h.

(15) Ricci, F.; Lai, R. Y.; Heeger, A. J.; Plaxco, K. W.; Sumner, J. J. *Langmuir* **2007**, *23*, 6827–6834.
(16) Du, H.; Strohsahl, C. M.; Camera, J.; Miller, B. L.; Krauss, T. D. *J. Am. Chem. Soc.* **2005**, *127*, 7932–7940.
(17) Jin, R. C.; Wu, G. S.; Li, Z.; Mirkin, C. A.; Schatz, G. C. *J. Am. Chem. Soc.* **2003**, *125*, 1643–1654.
(18) Frutos, A. G.; Pal, S.; Quesada, M.; Lahiri, J. *J. Am. Chem. Soc.* **2002**, *124*, 2396–2397.
(19) Aboul-ela, F.; Koh, D.; Tinoco, I.; Martin, F. H., Jr. *Nucleic Acids Res.* **1985**, *13*, 4811–4824.

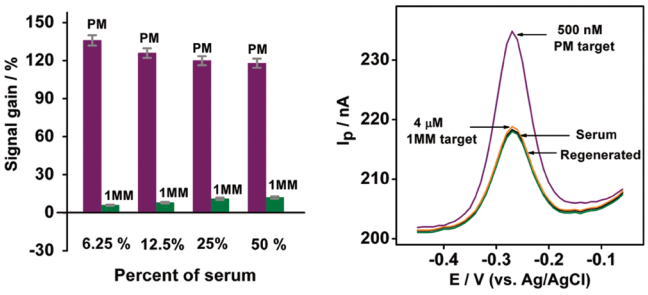

Figure 4. The E-SNP sensor retains its excellent discrimination capability even in complex sample matrices, such as blood serum. It is also easily regenerated, even after use in complex samples. (Left) A histogram representation of discrimination responses in various concentrations of diluted fetal calf serum doped with 500 nM 17-base perfectly matched target (PM; **2**) or 4 μM of a single-base mismatched target (1MM; **3**). (Right) The original AC voltammograms in 50% serum. After challenging the E-SNP sensor with target-doped serum, a 60 s wash in NaOH solution was sufficient to achieve 95% regeneration of the sensor. All hybridization reactions were performed in 300 μL of solution for 3 h.

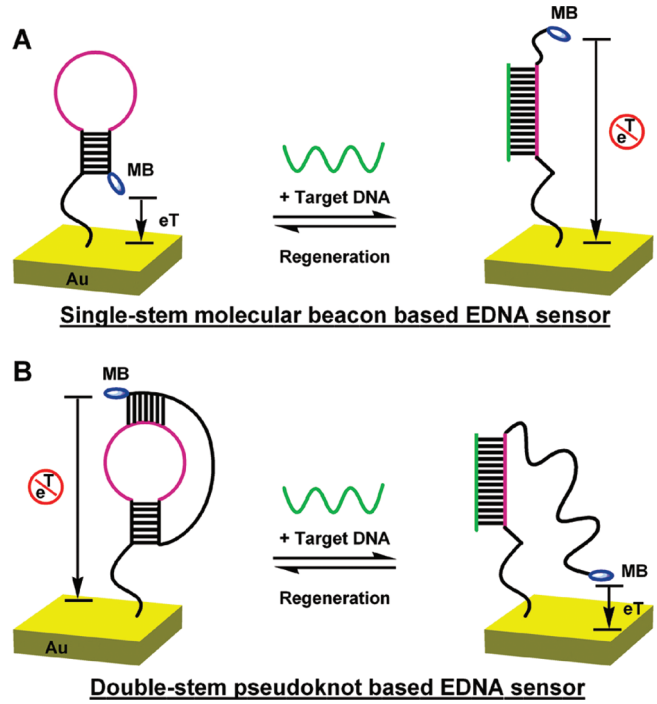

Figure 5. A schematic of the "signal-off" single-stem (molecular beacon) based and "signal-on" double-stem (pseudoknot) based electrochemical DNA (EDNA) sensors. Signal transduction is based on a binding-induced conformation change in a redox-tagged, electrode-bound probe. (A) In the absence of target, the molecular beacon structure holds the MB tag in close proximity to the electrode, allowing electron transfer. In the presence of complementary target, DNA hybridization forces the MB tag away from the electrode, limiting electron transfer and producing a detectable decrease in redox current. (B) The pseudoknot probe's structure holds the methylene blue tag away from the electrode without target, limiting electron transfer. Upon addition of a complementary target, the pseudoknot unfolds, allowing the redox tag to collide more freely with the electrode, thereby increasing the redox current.

experiments presumably arises due to hindered electron transfer in serum or serum-induced deviations in the salt concentration of our otherwise optimized hybridization buffer.

Sensor regeneration is critical to ascertain that observed signal gain is in fact due to specific target binding, which should be reversible. Because our probe is only a single DNA element covalently attached to the electrode surface, the E-SNP sensor is stable for convenient regeneration; a 60-s room temperature wash with 50 mM NaOH was sufficient to recover >95 $\pm$ 2% of the initial sensor signal, even for sensors previously used in 50% serum (Figure 4, right). Consistent with this, the E-SNP sensor can be regenerated more than five times with a mean recovery of >94% of the original signal before significant degradation is observed (see Supporting Information Figure S2).

The triple-stem probe based E-SNP sensor exhibits superior mismatch discrimination at room temperature compared to single-stem molecular beacon (Figure 5A) and double-stem pseudoknot (Figure 5B) based electrochemical sensors. For example, at target concentration of 200 nM, our original, "signal-off" sensor[22] based on a single-stem molecular beacon DNA probe produces discrimination factors of 1.4 and 3.4 for 3- and 5-base mismatches in a 17-base target, respectively.[11] A "signal-on" sensor based on a double-stem pseudoknot yields somewhat better mismatch discrimination:[11] using a pseudoknot probe composed of two fixed 7-bp stems and a poly (T) 3′ loop, we observed discrimination factors of 1.7 and 11 for single- and double-base mismatches out of a 17-base target concentration (at 200 nM).[12] In contrast, however, the triple-stem probe based E-SNP sensor shows maximum discrimination factors of 16 and 165 for single- and double-base mismatched targets.

We believe that the triple-stem probe's superior selectivity for mismatched bases at room temperature originates from the distinctive thermodynamic properties that are inherent in its structure. To elucidate this hypothesis, we constructed fluorophore/quencher-modified DNA probes designed to assume molecular beacon (**6**), pseudoknot (**7**), or triple-stem (**8**) structures. We determined the changes in enthalpy (ΔH) and entropy (ΔS) describing the phase transition between phase 2 (folded probe) and 3 (random coil) ($\Delta H_{2\rightarrow3}^0$ and $\Delta S_{2\rightarrow3}^0$) using van't Hoff plots[23,24] (see Supporting Information Figure S3) and from phase 1 (target-probe duplex) to phase 2 ($\Delta H_{1\rightarrow2}^0$ and $\Delta S_{1\rightarrow2}^0$) based on the linear relationship between the inverse of melting temperature ($1/T_m$) and $R \ln(T_0 - 0.5P_0)$ [ref 23] (Figure 6A). Although all of the probes tested here are conformationally constrained polymers, the rearrangement of the triple-stem probe upon target binding leads to larger enthalpy and entropy changes compared to those observed for the molecular beacon and pseudoknot probes. This observation is consistent with the melting temperatures (T_m) [ref 21] of the probes, which are 32.0, 45.4, and 80.2 °C for the molecular beacon, pseudoknot, and triple-stem probe, respectively. As evidence that elucidates the molecular origins of the improved specificity of the triple-stem probe, we obtained a 3-fold difference in $\Delta H_{1\rightarrow2}^0$ and $\Delta S_{1\rightarrow2}^0$ between triple-stem probe duplexes with PM and 1MM targets. In contrast, negligible differences were measured for such duplexes with molecular beacon and pseudoknot probes (Figure 6A, see table).

Using these values of ΔH and ΔS, we constructed free energy diagrams[23] of the three phases of the probes at equilibrium with

(20) Petruska, J.; Goodman, M. F. *J. Biol. Chem.* **1995**, *270*, 746–750.
(21) Kushon, S. A.; Jordan, J. P.; Seifert, J. L.; Nielsen, H.; Nielsen, P. E.; Armitage, B. A. *J. Am. Chem. Soc.* **2001**, *123*, 10805–10813.
(22) Fan, C. H.; Plaxco, K. W.; Heeger, A. J. *Proc. Natl. Acad. Sci. U.S.A.* **2003**, *100*, 9134–9137.
(23) Bonnet, G.; Tyagi, S.; Libchaber, A.; Kramer, F. R. *Proc. Natl. Acad. Sci. U.S.A.* **1999**, *96*, 6171–6176.
(24) Marky, L. A.; Breslauer, K. J. *Biopolymers* **1987**, *26*, 1601–1620.

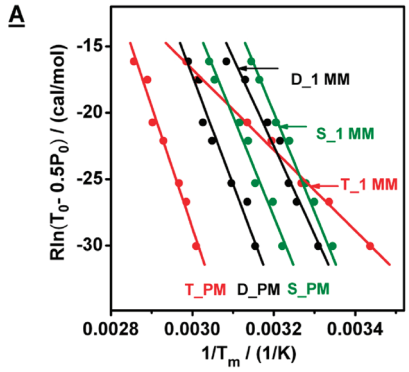

DNA probe/target duplex	Enthalpy ($\Delta H^0_{1\to2}$) (Kcal/mol)	Entropy ($\Delta S^0_{1\to2}$) (cal/mol·K)
Single-stem MB/PM duplex (S_PM)	73 ± 1	207± 2
Single-stem MB/1MM duplex (S_1 MM)	69 ± 1	200 ± 2
Double-stem probe/PM duplex (D_PM)	78 ± 1	217 ± 2
Double-stem probe/1MM duplex (D_1 MM)	64 ± 1	183 ± 2
Triple-stem probe/PM duplex (T_PM)	89 ± 1	242 ± 3
Triple-stem probe/1 MM duplex (T_1 MM)	30 ± 1	73 ± 3

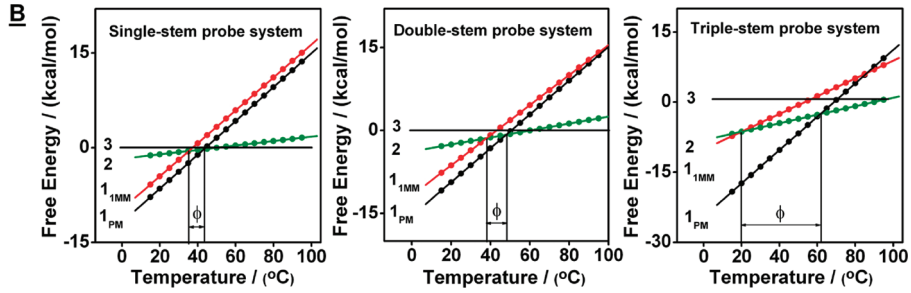

Figure 6. A comparative thermodynamic analysis among molecular beacon, pseudoknot, and triple-stem probes. (A) The thermodynamic parameters describing the dissociation of probe−target duplexes were determined by the increased melting temperature of the probe−target duplex. Separate determinations were performed with 17-base PM and 1MM targets (S = molecular beacon probe; D = pseudoknot probe; T = triple-stem probe). The calculated enthalpies and entropies are listed in the table. (B) Free energy diagrams of the three phases of the various probes in equilibrium with 17-base targets. The differences (Φ) between the melting temperature of PM duplexes (phase 1_{PM}) and 1MM duplexes (phase 1_{1MM}) for molecular beacon, pseudoknot, and triple-stem systems are 8.2, 10.2, and 42.1 °C, respectively. All hybridization reactions were performed in 300 μL of solution for 3 h.

their 17-base targets (Figure 6B). As expected, the triple-stem probe demonstrates a significantly larger temperature range for the transition from phase 1 to phase 2 between PM and 1MM targets[25] (19.9−62.0 °C; Φ = 42.1 °C) in comparison with those of the molecular beacon (35.0−43.2 °C; Φ = 8.2 °C) or pseudoknot probe (38.1−48.3 °C; Φ = 10.2 °C). From the total measured ΔH and ΔS in the three phases, it is clear that the triple-stem probe undergoes greater reorganization than the other probes upon dissociation (or formation) of probe−target duplexes and reformation of the dissociated probe. Thus, we believe that both the entropy gain and enthalpy loss to the free energy of the probe-target dissociated state, especially in the presence of a mismatched base pairing, lead to significantly improved specificity at room temperature.

Conclusions

Here we have demonstrated a reagentless and reversible electrochemical sensor capable of the single-step, room-temperature detection of single nucleotide polymorphisms (SNPs) directly in complex, clinically relevant samples. The sensor employs a single electrode-bound, methylene blue-modified, triple-stem DNA probe that provides exceptional specificity against single-based mismatches and effectively discriminates the 64 nM perfectly matched target in a sample containing a significant excess (4 μM) of single-base mismatched targets in 30 min at room temperature without exogenous reagents. By measuring the changes in enthalpy and entropy among different phases of target−probe states, we present the thermodynamic basis of the higher SNP specificity over previously reported molecular beacon and pseudoknot probes. From the experimental data, we observe that the triple-stem probe is superior in almost all respects of single-mismatch detection, with the possible exception of assay speed.

The current detection limit of the E-SNP sensor is ~5 nM (250 ng/μL), which is similar to those of molecular beacons and other hybridization probes. This level of sensitivity precludes, however, the direct detection of SNPs in genomic DNA in biological samples: the concentration of genomic DNA obtained from standard phenol/chloroform-based extractions is typically ~30 ng/μL, and biological samples typically contain long DNA fragments (e.g., kilobases), making direct detection of SNPs challenging.[26] To circumvent this problem, PCR or other amplification may be necessary; many traditional clinical assays use multiple PCR primers designed to flank mismatched base-containing regions that generate amplified targets of ~100−200 bp, and such sample preparation strategies would be well suited for the E-SNP sensor.

Importantly, we note that the design of the triple-stem probe requires negligible sequence optimization to achieve the highly specific SNP detection reported here. Given the observation that any oligonucleotide probe can be designed to form triple-stem structures through Watson−Crick base pairing,[27] combined with the fact that labeled DNA can be immobilized on a solid phase without significant loss of affinity,[28] it appears that the E-SNP

(25) Xiao, Y.; Plakos, K. J. I.; Lou, X. H.; White, R. J.; Qian, J. R.; Plaxco, K. W.; Soh, H. T. *Angew. Chem., Int. Ed.* **2009**, *48*, 4354–4358.
(26) Tsourkas, A.; Behlke, M. A.; Rose, S. D.; Bao, G. *Nucleic Acids Res.* **2003**, *31*, 1319–1330.
(27) Pleij, C. W. A.; Rietveld, K.; Bosch, L. *Nucleic Acids Res.* **1985**, *13*, 1717–1731.
(28) Bock, L. C.; Griffin, L. C.; Latham, J. A.; Vermaas, E. H.; Toole, J. J. *Nature* **1992**, *355*, 564–566.

sensor may provide a useful approach toward highly multiplexed clinical diagnostics at the point-of-care.

Experimental Section

Materials. All chemicals, including 6-mercaptohexanol, tris(2-carboxyethyl) phosphine hydrochloride (TCEP) and fetal calf serum (from formula-fed bovine calves, USA origin, sterile-filtered, cell culture-tested and iron-supplemented) were purchased from Sigma-Aldrich, Inc. (St. Louis, MO) and used as received without further purification. Our thiolated, methylene blue (MB)-labeled DNA probes, as well as our fluorophore (Cal Fluor 610)/quencher (BHQ)-modified molecular beacon, pseudoknot, and triple-stem probes, were synthesized and purified by Biosearch Technologies, Inc. (Novato, CA) and confirmed by mass spectrometry. The sequences of the modified probes are as follows:

(**1**) 5′-HS-$(CH2)_{11}$- AGGCTGGATTTTTTATTTACCTTTTTT-TAGGTAAAACGACGGCCAG CCTTTTTTTTTTTTTCCGTCGT-$(CH2)_7$-MB-3′

(**5**) 5′-HS-$(CH2)_{11}$-AGGCTGGATTTTTTATTTACCTTTTTT-TAGGTAAAACGGCGGCCAG CCTTTTTTTTTTTTTCCGTCGT-$(CH2)_7$-MB-3′

(**6**) 5′-(Cal Fluor 610)-AGGCTGGAGGTAAAACGACGGC-CAGCCT-(BHQ)-3′

(**7**) 5′-GGCGAGGTAAAA-(BHQ)-CGACGGCCAGCCTCGC-CGTTTTTTTTTTTTTTTTGC CGTCG-T-(Cal Fluor 610)-3′

(**8**) 5′-AGGCTGGATTTTTTATTTACCTTTTTTTAGGTAAAA-(BHQ)-CGACGGCCAGCC TTTTTTTTTTTTTCCGTCGT-(Cal Fluor 610)-3′

Our target oligonucleotides were purchased from Integrated DNA Technologies Inc. (Coralville, IA) and were purified by HPLC. The sequences of these targets, with mismatch locations in red, are as follows:

15-mer DNA targets: PM target: 5'-CTGGCCGTCGTTTTA-3';

1MM target: 5'-CTGGCCGTAGTTTTA-3'

17-mer DNA targets: PM target: (**2**) 5'-GCTGGCCGTCGTTTTAC-3'

1MM target: (**3**) 5'-GCTGGCCCTCGTTTTAC-3'

2MM target: (**4**) 5'-GCTGGCCCCCGTTTTAC-3'

19-mer DNA targets: PM target: 5'-GGCTGGCCGTCGTTTTACC-3'

1MM target: 5'-GGCTGGCCCTCGTTTTACC-3'

Gold Electrode Cleaning and E-SNP Sensor Preparation. The sensors were fabricated on polycrystalline gold disk electrodes (1.6-mm diameter; BAS, West Lafayette, IN). The electrodes were prepared by polishing with 1.0 μm diamond and 0.05 μm alumina (BAS) suspensions, followed by sonication in water and multiple steps of electrochemical cleaning, as described elsewhere in the literature.[29] After cleaning, the electrodes were modified with the probe DNA by immersion in a 0.2 μM solution (300 μL) of the thiolated MB-labeled DNA oligomer (**1**) in a high salt phosphate buffer (100 mM sodium phosphate including 1.5 M NaCl and 1 mM Mg^{2+} (pH = 7.2)) for 16 h at room temperature. Prior to immobilization, the probe DNA was incubated for 1 h in 2 μM TCEP to reduce disulfide bonds. After probe immobilization, the electrode surface was rinsed with deionized water and then passivated by immersion in 1 mM 6-mercaptohexanol in phosphate buffer for 4 h at room temperature. The electrodes were rinsed again with deionized water and stored in 1 mM phosphate buffer (pH = 7.0, including 1 mM NaCl and 30 mM Mg^{2+}) prior to measurements.

Varied Surface Coverage of Triple-Stem Probe on the Electrode. Electrodes and probes were prepared independently as described above. After cleaning, the electrodes were then modified with the triple-stem DNA probe by immersion in a 5, 1, 0.2, 0.01, or 0.001 μM solution of the reduced, thiolated MB-labeled DNA oligomer (**1**) in 300 μL of high salt phosphate buffer (100 mM phosphate, 1.5 M NaCl, 1 mM Mg^{2+}, pH = 7.2) for 16 h at room temperature. Different DNA probe concentrations employed during electrode fabrication produced different surface coverages of the triple-stem probes.

Electrochemical Measurements. All measurements were performed by alternating-current voltammetry (ACV) with a CHI 603 potentiostat (CH Instruments, Austin, TX) in a standard cell (a platinum wire as counter electrode and an Ag/AgCl electrode as reference electrode). E-SNP sensor measurements were conducted by monitoring the electrode in the hybridization buffer (2 mL), which includes 1 mM phosphate, 1 mM NaCl, and 30 mM Mg^{2+} (pH = 7.0). This hybridization buffer was used in all our experiments because the E-SNP sensor gave strong and stable discrimination signals against single-mismatched targets both in this buffer alone and in a mixture with serum. SNP detection was carried out either in the hybridization buffer or in fetal calf serum diluted to 6.25%, 12.5%, 25%, and 50% in buffer where the salt concentration was varied to control the pH and ionic strength and thereby obtain the same final salt concentration as that in pure hybridization buffer. With the exception of the time-course experiments, the sensors were incubated in each sample for 3 h at room temperature before being monitored using the ACV with a step potential of 10 mV, amplitude of 25 mV, and frequency of 10 Hz. The E-SNP sensors were regenerated by a simple 30 s, 50 mM NaOH rinse at room temperature.

Determination of Melting Temperatures (T_m). Fluorescence melting curves of the single-stem molecular beacon (**6**), double-stem pseudoknot (**7**), and triple-stem (**8**) probes were measured at 610 nm with a Varian Cary 100 spectrometer (Palo Alto, CA) equipped with a Peltier block. The probe and 17-base target oligonucleotides were mixed at a 1:1 ratio (v/v) and allowed to hybridize in a degassed hybridization buffer for 3 h at room temperature, with the solutions adjusted to a final volume of 100 μL. Prior to analysis, the samples were heated to a maximum temperature of 95 °C for 10 min and then cooled to the starting temperature of 20 °C. Melting curves were recorded at a rate of 1.0 °C/min, from 20 to 100 °C, with each step lasting 5 min. The T_m's were determined through a standard method[23] in which we fit all the data in each thermal denaturation profile to eq 3. Before denaturation experiments, cuvettes were calibrated to obtain the same probe fluorescence intensity for all samples.

Acknowledgment. This work was supported by the Office of Naval Research, National Institutes of Health, and Institute for Collaborative Biotechnologies through the U.S. Army Research Office.

Supporting Information Available: Alternating current voltammograms of the E-SNP sensor against different targets, the specificity and stability of the E-SNP sensor, and determination and calculation of thermodynamic parameters of single-stem probe, double-stem probe, and triple-stem probes. This material is available free of charge via the Internet at http://pubs.acs.org.

JA905068S

(29) Xiao, Y.; Lai, R.; Plaxco, K. W. *Nat. Protoc.* **2007**, *2*, 2875–2880.